

## Chapter 1 Introduction

### Contents

1.1. Magnetic moments and magnetic fields . . . . .	1
1.2. About the spin moments . . . . .	4
1.3. Something more about the nuclear spin . . . . .	8
1.4. A lot more about the electron spin . . . . .	9
1.5. About the energies . . . . .	14
1.6. Magnetization and magnetic susceptibility . . . . .	15
1.7. The nuclear magnetic resonance experiment . . . . .	18
1.7.1. The continuous wave experiment and definition of $T_1$ and $T_2$ . . . . .	18
1.7.2. The pulse experiment . . . . .	20
1.7.3. The chemical shift . . . . .	22
1.7.4. Something more about relaxation rates . . . . .	24
References . . . . .	27
General references . . . . .	27

### 1.1. Magnetic moments and magnetic fields

This book will deal with NMR experiments on systems which contain unpaired electrons. Unpaired electrons disturb the experiment to such an extent that quite different conditions are needed. However, since we have to live with molecules bearing unpaired electrons, we do our best to take advantage from these newly designed NMR experiments in order to learn as much as possible regarding the properties of the unpaired electrons and the structure and dynamics of the substance. To be more precise, we are going to exploit NMR in order to learn how the unpaired electron(s) interacts with the resonating nucleus and how these perturbed nuclei provide information typical of NMR experiments.

The nucleus under investigation must have a magnetic moment in order to make the NMR experiment possible. An unpaired electron also has a magnetic moment. A magnetic moment  $\mu$  ( $\text{J T}^{-1}$ ) can be visualized as a magnetic dipole (Fig. 1.1). Such magnetic moment causes a magnetic dipolar field. In electromagnetism, this vector is provided by a continuous current in a coil (Fig. 1.2). If a second magnetic moment  $\mu_2$  (which we take to be of smaller vector intensity without loss of generality) is within the dipolar field created by the former magnetic moment  $\mu_1$  anchored at a distance  $r$ , it will orient accordingly, as represented in Fig. 1.3. We can refer to the electronic magnetic moment as the large magnetic moment  $\mu_1$  and to the nucleus as

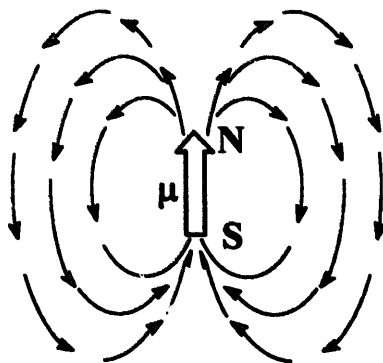


Fig. 1.1. A magnetic moment can be seen as a magnetic dipole characterized by north and south polarities. It gives rise to a magnetic field which is indicated by force lines. The dipolar nature provides the vectorial nature of this moment, whose intensity is indicated by  $\mu$ .

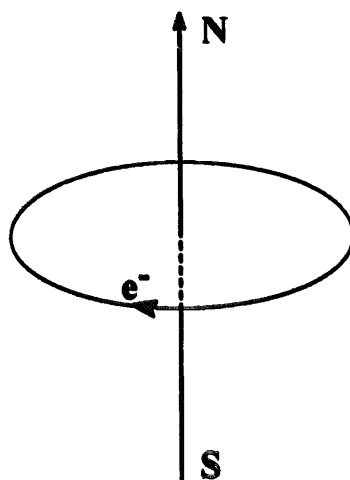


Fig. 1.2. A continuous flow of electricity in a coil provides a magnetic moment which is proportional to the intensity of the current and depends on the coil size.

the small magnetic moment  $\mu_2$ . The absolute value of the magnetic moment associated with the electron is 658 times that for a proton, which has the largest magnetic moment among the magnetic nuclei (except tritium). The orientation of the small magnetic moment along the dipolar field of the large magnetic moment shown in Fig. 1.3 represents the minimum energy situation. In general, the energy of the interaction between the two magnetic bars depends on the relative orientation of the two vectors, if fixed by external forces, according to Eq. (1.1):

$$E^{\text{dip}} = -\frac{\mu_0}{4\pi} \left[ \frac{3(\mu_1 \cdot r)(\mu_2 \cdot r)}{r^5} - \frac{\mu_1 \cdot \mu_2}{r^3} \right] \quad (1.1)$$

where  $\mu_0$  is the magnetic permeability of a vacuum,  $r$  is the vector connecting the two point dipoles and  $r$  is its magnitude. The energy can be negative (stabilization)

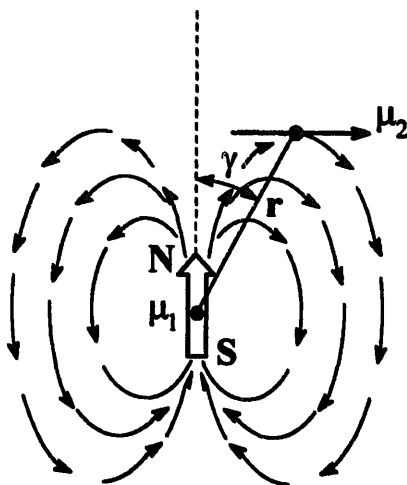


Fig. 1.3. Orientation of a small magnetic moment  $\mu_2$  (e.g. that of the nucleus) within a magnetic field generated by a larger magnetic moment  $\mu_1$  (e.g. that of the electron) at distance  $r$ . Here  $\gamma$  is the angle between  $\mu_1$  and  $r$ .

or positive (destabilization) according to the relative magnitude of the two terms in parentheses.

In all our experiments the two magnetic bars are immersed in an external magnetic field. The intensity of the magnetic field is proportional to the density of force lines (Fig. 1.4). Later, we will be interested in the effective field in a given region of space, which is referred to as magnetic induction  $B$  (expressed in tesla):

$$B = \mu_0(H + M) = B_0 + \mu_0 M \quad (1.2)$$

where  $H$  and  $M$  ( $\text{J T}^{-1} \text{m}^{-3}$ ) are the magnetic field strength and the magnetization of the medium referred to unit volume respectively, and  $\mu_0$  ( $\text{J}^{-1} \text{T}^2 \text{m}^3$ ) is already defined (Eq. (1.1)). The magnetic induction is thus given by the magnetic induction in a vacuum ( $\mu_0 H = B_0$ ) plus a contribution ( $\mu_0 M$ ) depending on the kind of sub-

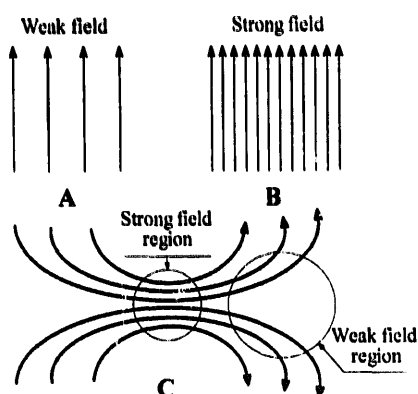


Fig. 1.4. The force lines of a magnetic field  $B_0$ . (A) A weak, homogeneous field. (B) A strong, homogeneous field. (C) An inhomogeneous field with weak and strong field regions.

stance constituting the medium. In this book, the magnetic induction in a vacuum  $B_0$  will always be referred to as the *external magnetic field*.

The energy  $E$  of a magnetic moment  $\mu$  immersed in a magnetic field  $B_0$  is given by

$$E = -\mu \cdot B_0 \quad (1.3)$$

Eq. (1.3) shows that the energy is at a minimum when  $\mu$  is aligned along  $B_0$ .

In the absence of further limit conditions which may hold in the case of the electron (see later), we can now think of an electron spin and a nuclear spin anchored at points A and B, both aligned along the external magnetic field  $B_0$ , as shown in Fig. 1.5. Since the two magnetic moments are forced to be parallel by the strong external field, the energy of the interaction between them, given by Eq. (1.1), simplifies to

$$E^{\text{dip}} = -\frac{\mu_0}{4\pi} \frac{\mu_1 \mu_2}{r^3} (3 \cos^2 \gamma - 1) \quad (1.4)$$

where  $\gamma$  is the angle between the direction of  $B_0$  and that of the AB vector.

## 1.2. About the spin moments

Electron and nuclear magnetic moments can be regarded as arising from a property of the particles, i.e. that they possess an angular momentum as if they were spinning. Such angular momenta are given by

$$J_s = hS \quad J_I = hI \quad (1.5)$$

for the electron and nucleus respectively, where  $S$  and  $I$  are dimensionless *spin* angular momentum vectors and  $h = h/2\pi$  is the Planck constant ( $\text{J s rad}^{-1}$ ). The

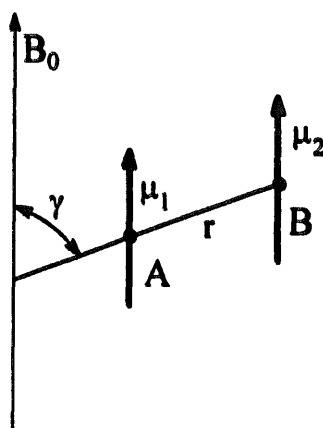


Fig. 1.5. Two magnetic bars,  $\mu_1$  and  $\mu_2$ , anchored at generic points A and B at distance  $r$  in a magnetic field  $B_0$ ,  $\gamma$  is the angle between the magnetic field and the AB vector.

moduli of the vectors are given by

$$J_S = h\sqrt{S(S+1)} \quad J_I = h\sqrt{I(I+1)} \quad (1.6)$$

where  $S$  and  $I$  are quantum numbers associated with the spinning particle. For a single electron or for a single nucleon (proton or neutron),  $S = I = \frac{1}{2}$ .  $S$  or  $I$  identify sets of spin wavefunctions for the above particles. Note that the values of the angular momenta are not related to the nature of the particles.

The eigenvalues corresponding to these wavefunctions along a  $z$  direction (defined by an external magnetic field or otherwise) are  $+\frac{1}{2}$  or  $-\frac{1}{2}$  (Fig. 1.6). Thus we have two wavefunctions, one with  $S$  (or  $I$ )  $= \frac{1}{2}$  and with a component along  $z = \frac{1}{2}$  and another with  $S$  (or  $I$ )  $= \frac{1}{2}$  and with a component along  $z = -\frac{1}{2}$ .

The component is indicated in quantum mechanics as  $M_S$  or  $M_I$ . The notation to indicate the wavefunction is thus

$$|S, M_S\rangle \quad \text{or} \quad |I, M_I\rangle$$

where  $|\rangle$  is the “ket” notation for wavefunctions.

These wavefunctions are eigenfunctions of the operators  $S^2$  ( $I^2$ ) and  $S_z$  ( $I_z$ ).

$$\begin{aligned} S^2|S, M_S\rangle &= S(S+1)|S, M_S\rangle \\ I^2|I, M_I\rangle &= I(I+1)|I, M_I\rangle \\ S_z|S, M_S\rangle &= M_S|S, M_S\rangle \\ I_z|I, M_I\rangle &= M_I|I, M_I\rangle \end{aligned} \quad (1.7)$$

Physically, it means that it is possible to know simultaneously the square of the

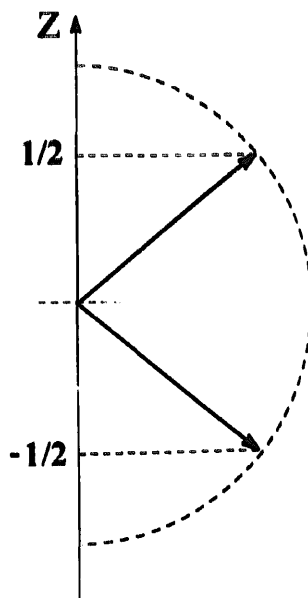


Fig. 1.6. Allowed orientations of an  $I = \frac{1}{2}$  angular momentum relative to the  $z$  direction defined by the external magnetic field. The vector has modulus  $\sqrt{3}/2$ , and its projections on the  $z$  axis are  $\frac{1}{2}$  and  $-\frac{1}{2}$ .

intensity of the spin angular momentum and its component along  $z$ . Since the spin wavefunctions are not eigenfunctions of the operators  $S$  or  $I$ , it is impossible to know intensity and orientation of the angular momentum vector. We will learn how to live with it!

Since the electron and the proton are charged particles, there is a magnetic moment associated with the angular momenta. The latter is related to a motion, and a motion of a charged particle produces a magnetic moment. The neutron is not charged as a result of balancing of charges of different sign. However, since the charges are not homogeneously distributed from the center of the particle, the neutron also has a magnetic moment associated with the angular momentum.

There is a proportionality between angular momenta and magnetic moments, the moduli of the latter being given by

$$|\mu_S| = |g_e| \frac{|e|\hbar}{2m_e} \sqrt{S(S+1)} = |g_e| \mu_B \sqrt{S(S+1)} \quad (1.8)$$

$$|\mu_I| = |g_I| \frac{|e|\hbar}{2m_p} \sqrt{I(I+1)} = |g_I| \mu_N \sqrt{I(I+1)} \quad (1.9)$$

where  $e$  is the elementary charge of the electron,  $g_e$  is the so-called free electron  $g$  value, which is 2.0023<sup>1</sup>.  $\mu_B$  and  $\mu_N$  are the electron Bohr magneton and nuclear magneton,  $m_e$  and  $m_p$  are the electron and proton masses, and  $g_I$  depends on the nucleus under consideration (see later). The ratio of  $|\mu_S|$  and  $|\mu_I|$  for the proton is 658.2107 [1]. Analogously to the angular momenta, only the projection along  $z$  of the magnetic moment and its modulus are known, but not its direction.

Sometimes the magnetogyric ratio  $\gamma$  is used to indicate the ratio between magnetic moments and angular momenta.

$$\gamma_S = -\frac{g_e \mu_B}{\hbar} \quad \gamma_I = \frac{g_I \mu_N}{\hbar} \quad (1.10)$$

where  $\gamma_S$  and  $\gamma_I$  for the proton have opposite signs, their ratio thus being  $-658.2107$ .

If reference is made to Fig. 1.7, it appears that the angle  $\varphi$  is known because the modulus of vector  $\mu$  is known, as well as its projection along the  $z$  axis, but the orientation of  $\mu$  cannot be known.

$$\mu_z = \mu \cos \varphi \quad (1.11)$$

This nicely reconciles the quantum-mechanical picture with classical physics, which shows that a magnetic moment which must form an angle  $\varphi$  with the direction of an external magnetic field *precesses* about it with an angular frequency

$$\omega = -\gamma B_0 \quad (1.12)$$

The resulting picture of a spin moment (magnetic or angular) in a magnetic field

<sup>1</sup> In this book  $g_e$  is taken positive, and the equations containing  $g_e$  are explicitly written in such a way as to contain a positive  $g_e$ .

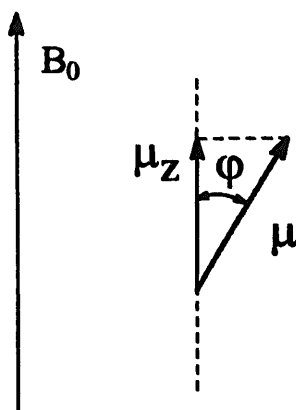


Fig. 1.7. A magnetic moment  $\mu$  in a magnetic field forming an angle  $\varphi$  with the magnetic field direction.

$B_0$  is that it precesses about the  $B_0$  direction with an angular frequency proportional to the intensity of  $B_0$  and to its own magnetic moment, and with the  $\varphi$  angles such that the projection of  $\mu$  along  $B_0$  assumes the quanto-mechanically allowed values  $\pm\mu_z$  (Fig. 1.8). The sign of  $\omega$ , which is related to the sign of  $g$  (Eqs. (1.10) and (1.12)), gives the direction of precession.

In the case of more than one unpaired electron the total spin value  $S$  is  $\frac{1}{2}$  times the number of unpaired electrons. Commonly, we will deal with one to seven unpaired electrons and  $S$  can thus take values from  $\frac{1}{2}$  to  $\frac{7}{2}$ .

In the case of odd numbers of protons and/or neutrons, a total spin value  $I$  varying from  $\frac{1}{2}$  to 7 occurs. Owing to the complex intranuclear forces, the  $g_I$  values also vary from 5.96 for  $^3\text{H}$  to 0.097 for  $^{191}\text{Ir}$ . The  $g_I$  values for magnetically active nuclei are summarized in Appendix I.

The number of allowed values of  $M_S$  (or  $M_I$ ) is  $2S + 1$  (or  $2I + 1$ ), and the values range from  $S$  to  $-S$  (or from  $I$  to  $-I$ ), differing by one unit. Fig. 1.9 shows the allowed orientations for a spin  $S = 2$  (or  $I = 2$ ). It is just an extension of the  $I = S = \frac{1}{2}$  case.

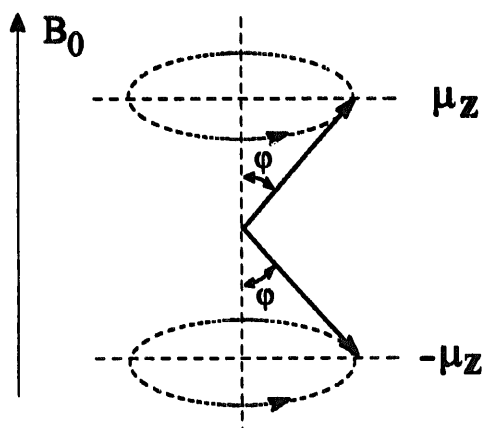


Fig. 1.8. The allowed precessions of a spin  $I = \frac{1}{2}$  with negative  $\gamma$  (positive  $\omega$ ) in a magnetic field.

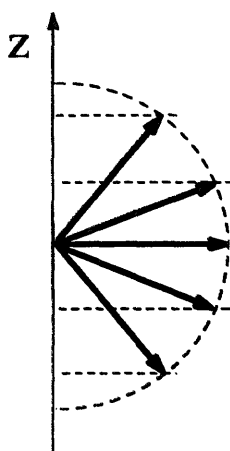


Fig. 1.9. Allowed orientations and  $z$  projections of a spin  $S = 2$  (or  $I = 2$ ) in a magnetic field.

### 1.3. Something more about the nuclear spin

Nuclear spin vectors are localized on the nucleus, at least for the purposes discussed here. Therefore they can be treated as point dipoles. We have already shown that they are described by  $2I + 1$  wavefunctions, each characterized by the value  $I$  and a value of  $M_I$ . We have already seen how they behave in a magnetic field.

We want now to point out that the different spin orientations in a magnetic field correspond to different energies. This is quite intuitive by looking at Fig. 1.9. If the orientation of the magnetic spin dipole is different in a magnetic field from case to case, then the interaction energies will be different. Actually, according to Eq. (1.3), the energy will be given by the product of the projection along  $z$  of the spin magnetic moment and the external magnetic field.

$$E = -g_I \mu_N M_I B_0 \quad (1.13)$$

where  $g_I \mu_N M_I$  is the projection of the spin magnetic moment along  $B_0$ .

In quantum mechanical terms the energy is given by the Hamiltonian operator, which in this case is called the nuclear Zeeman Hamiltonian

$$\mathcal{H} = -g_I \mu_N \mathbf{I} \cdot \mathbf{B}_0 \quad (1.14)$$

where  $\mathbf{I}$  is the spin operator. Now, generally the nuclear spin vectors have the  $z$  axis along  $B_0$  and they have zero time average in the  $xy$  plane. Therefore, we can write

$$\mathcal{H} = -g_I \mu_N B_0 I_z \quad (1.15)$$

Since the application of  $I_z$  on a wavefunction  $|I, M_I\rangle$  gives  $M_I$  (Eq. (1.7)), the energies of interaction between the spin and the magnetic field given in Eq. (1.13) are obtained. Such energies are dependent on the magnitude of the external magnetic field (see Fig. 1.10) and the energy separation  $\Delta E$  between two adjacent levels is

$$\Delta E = g_I \mu_N B_0 (M_I - (M_I - 1)) = g_I \mu_N B_0 \quad (1.16)$$

In the absence of an external magnetic field the Zeeman operator provides zero energy and all the  $|I, M_I\rangle$  levels (termed as  $I$  manifold) have the same energy.



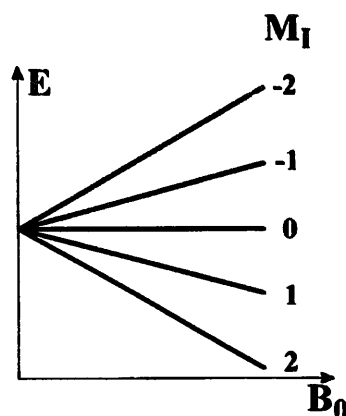


Fig. 1.10. The Zeeman energies of a nuclear spin ( $I = 2$ ) as a function of the external magnetic field  $B_0$ .

However, this may not be true for nuclei with  $I > \frac{1}{2}$ . In this case, the non-spherical distribution of the charge causes the presence of a quadrupole moment. Whereas a dipole can be described by a vector with two polarities, a quadrupole can be visualized by two dipoles as in Fig. 1.11.

The presence of a quadrupole moment can make the  $|I, M_I\rangle$  levels inequivalent even in the absence of an external magnetic field, provided there is an electric field gradient. Only the wavefunctions with the same absolute value of  $M_I$  are pairwise degenerate in axial symmetry, i.e.  $M_I = \pm 1, \pm 2$ , etc. An example is reported in Fig. 1.12 for  $I = \frac{3}{2}$ .

#### 1.4. A lot more about the electron spin

At variance with the nucleus, the electron is associated with an orbital, i.e. a wavefunction which is related to the distribution in space of the electron cloud, and which displays an angular momentum and a magnetic moment.

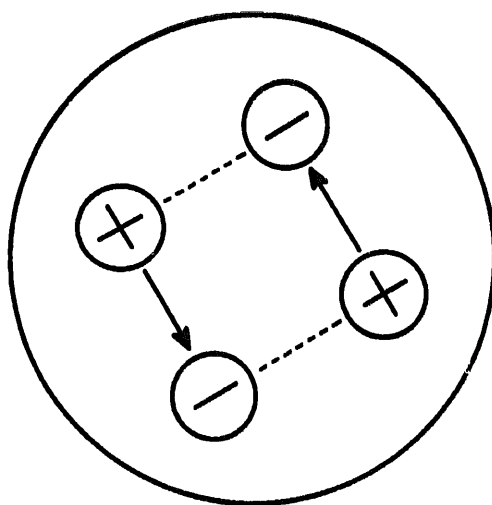


Fig. 1.11. Schematic drawing of a quadrupole moment.

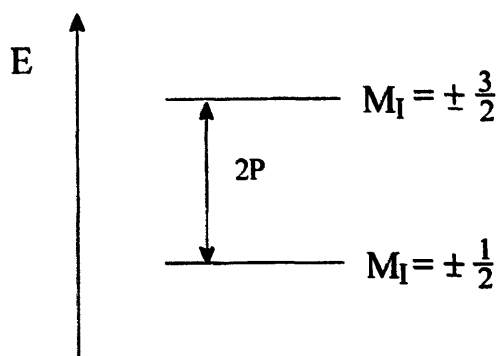


Fig. 1.12. The energy levels of a spin  $I = \frac{3}{2}$  at zero magnetic field in axial symmetry, with  $P$  being the product of the quadrupole moment with the electric field gradient.

In a naive and incorrect way we can say that the electron with  $S = \frac{1}{2}$  senses the orbital magnetic moment. Actually, a charged particle cannot sense the orbital magnetic moment due to its own movement. However, the electron moves in the electric potential of the charged nucleus. If we change the system of reference, the movement of the electron around the nucleus can be seen as a movement of the nucleus around the electron (Fig. 1.13). The “motion” of the charged nucleus then generates a magnetic moment which is sensed by the electron. A convenient way to describe the relative movement of the nucleus with respect to the electron is that of using the same  $n$ ,  $l$  and  $m_l$  quantum numbers describing the electron. The resulting angular and magnetic properties will depend on the values of  $m_s$  for the spin,  $m_l$  for the orbital, and on their interaction. The latter phenomenon is called *spin-orbit coupling* and is of paramount importance in understanding the electronic properties. Traditionally, two different formalisms are used for transition metal ions of the first series on one side and lanthanides on the other. In the latter case spin-orbit coupling is strong, and  $l$  and  $m_l$  are not good quantum numbers. This case will be treated later (see Chapter 2). In the former case, spin-orbit coupling is small enough to be considered a further perturbation. For more than one unpaired electron, total  $L$  and

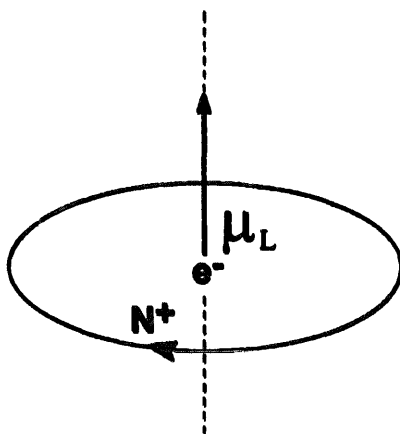


Fig. 1.13. The electron “senses” the orbital magnetic moment.

$M_L$  can be defined. In a molecule, the ligand field defines internal direction(s) along which the orbital angular momentum is preferentially aligned (quantized). Other orientations have higher energies.

Let us now interact the molecule with an external magnetic field  $\mathbf{B}_0$ . The interaction energy, as far as the orbital is concerned, is given by the orbital Zeeman operator

$$\mathcal{H} = \mu_B \mathbf{L} \cdot \mathbf{B}_0 \quad (1.17)$$

This interaction will tend to disalign  $\mathbf{L}$  from its internal axes (Fig. 1.14(A)). As a result, when the molecule rotates with respect to  $\mathbf{B}_0$ , the interaction energy of Eq. (1.17) is orientation dependent.

In coordination chemistry, reference is often made to limiting cases in which the orbital contribution tends to zero. In this case, the treatment is equal to the nuclear case and the same Hamiltonian is used (the opposite sign with respect to Eq. (1.14) is justified by the positive  $g_e$ ).

$$\mathcal{H} = g_e \mu_B \mathbf{S} \cdot \mathbf{B}_0 \quad (1.18)$$

and

$$E = g_e \mu_B M_S B_0 \quad (1.19)$$

In such a system, the external magnetic field defines the molecular  $z$  axis. If we rotate the molecule with respect to  $\mathbf{B}_0$ , the spin and its magnetic moment are not affected (Fig. 1.14(B)). However, in the molecule of Fig. 1.14(A), a molecular  $z$  axis can be

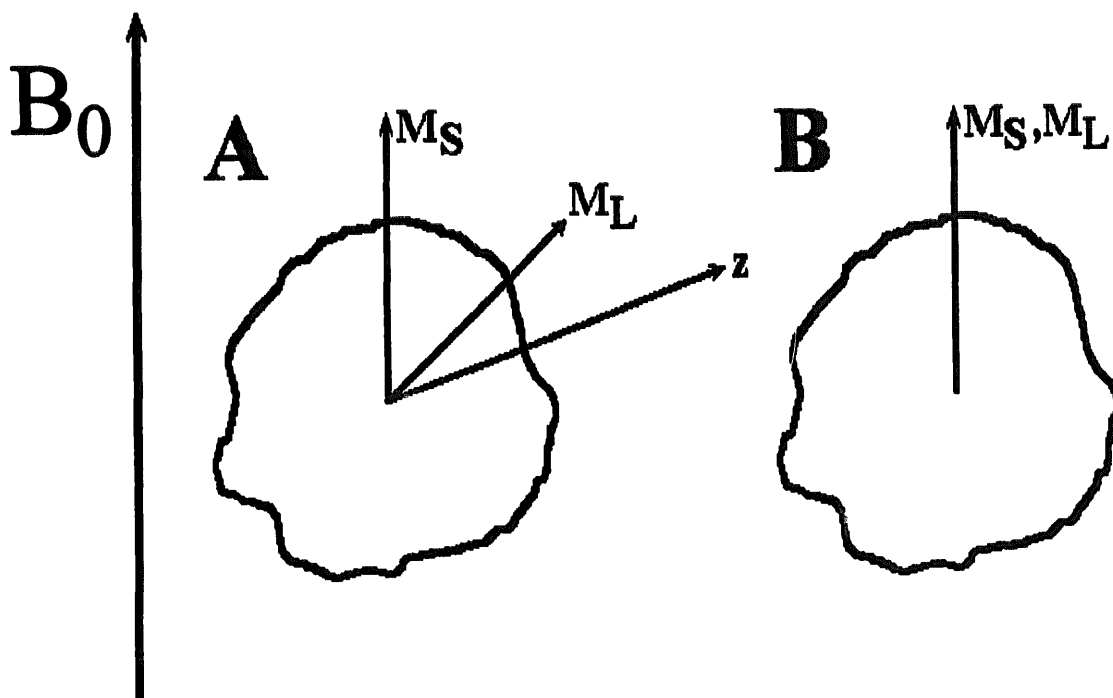


Fig. 1.14. (A) Orientation of  $M_S$  and  $M_L$  in the presence of internal molecular axes. (B) A case in which the external magnetic field determines the quantization axes.

defined. When rotating the molecule, the orbital contribution to the overall magnetic moment changes, whereas the spin contribution is constant. The total Zeeman Hamiltonian is

$$\mathcal{H} = \mu_B(\mathbf{L} + g_e\mathbf{S}) \cdot \mathbf{B}_0 \quad (1.20)$$

A convenient way to handle Eq. (1.20) is that of defining a tensor  $\mathbf{g}$  which couples the magnetic moment  $\mathbf{S}$  with the external magnetic field. Such a tensor defines the coupling between  $\mathbf{S}$  and  $\mathbf{B}_0$  for all molecular directions. We can represent the tensor as a solid ellipsoid (Fig. 1.15) with three principal directions defining the axes of the ellipsoid. In any  $kk$  direction we have a value of  $g_{kk}$  such that

$$g_{kk}^2 = g_{xx}^2 \cos^2 \alpha + g_{yy}^2 \cos^2 \beta + g_{zz}^2 \cos^2 \gamma \quad (1.21)$$

where  $\cos \alpha$ ,  $\cos \beta$  and  $\cos \gamma$  are the direction cosines of the  $kk$  vector. The energy

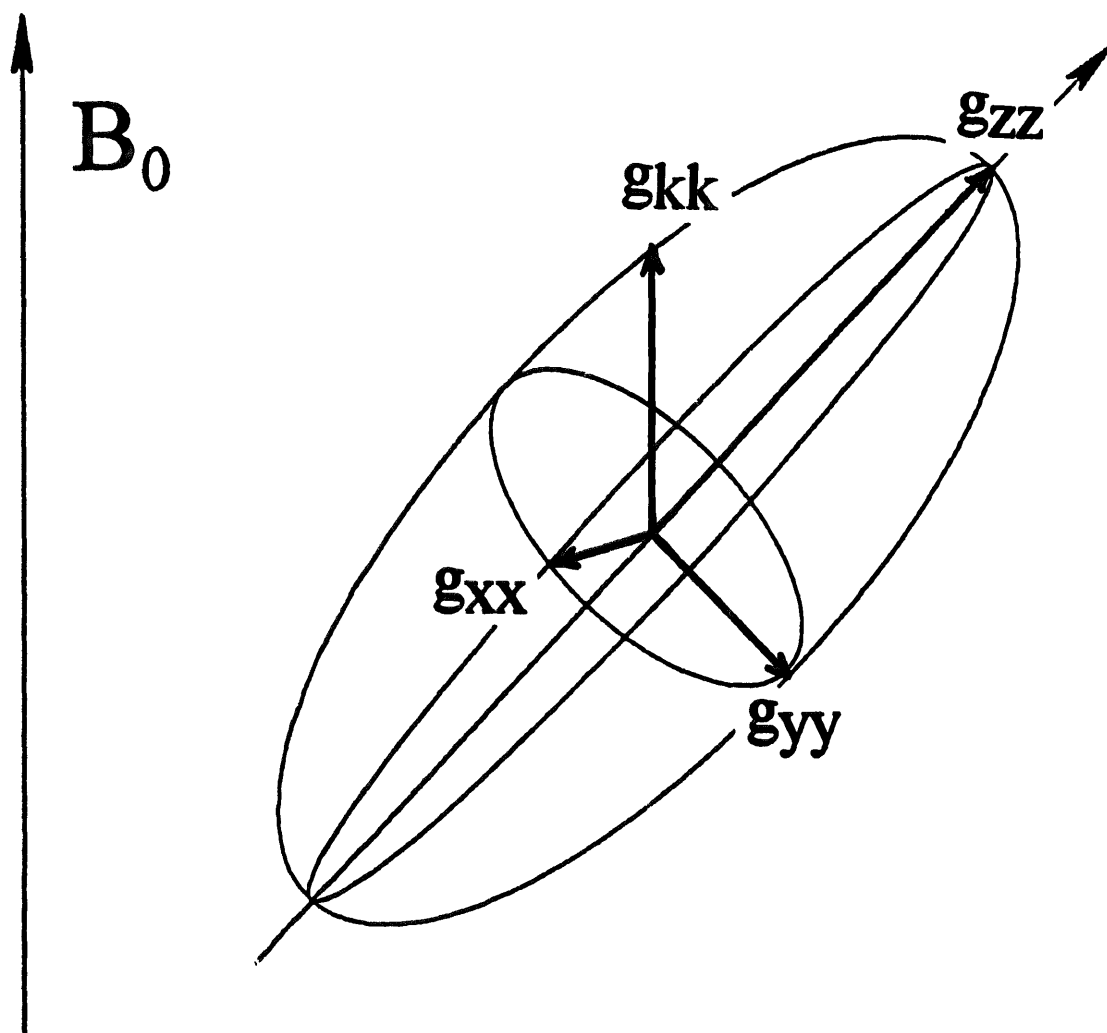


Fig. 1.15. The ellipsoid representing the components of the  $\mathbf{g}$  tensor in every direction. The molecule to which the tensor is associated has a generic orientation in the magnetic field  $\mathbf{B}_0$ .

of the  $|S, M_S\rangle$  function, when the magnetic field is along the  $kk$  direction, is

$$E = \mu_B g_{kk} M_S B_0 \quad (1.22)$$

As we can see, the expression of the energy does not contain  $L$ . The Hamiltonian has the form

$$\mathcal{H} = \mu_B \mathbf{S} \cdot \mathbf{g} \cdot \mathbf{B}_0 \quad (1.23)$$

which is the scalar product of the  $\mathbf{S}$  vector (defined in Section 1.2), the  $\mathbf{g}$  tensor and the  $\mathbf{B}_0$  vector.

This new formalism, known as spin-Hamiltonian formalism, does not contain the  $L$  operator, which would require more laborious calculations. Its effects are parametrically included in the  $\mathbf{g}$  tensor, which would pass from ellipsoidal to spherical in the absence of orbital angular momentum.

The projections of the total electron magnetic moment along any  $kk$  direction defined by  $\mathbf{B}_0$  are given by  $\mu_B g_{kk} M_S$ .

When the molecule under investigation rotates fast with respect to the  $g$  anisotropy (i.e. the reorientation rate  $\tau_r^{-1}$  (see also Section 3.2) is larger than the spreading of the different orientation-dependent energies of the spin ( $\tau_r^{-1} > \Delta E/h$ )) we measure an average  $g$  value  $\bar{g}$ , which is also different from  $g_e$ . The two limit situations of isotropic and anisotropic  $g$  are illustrated in Fig. 1.16. When  $g = 2.0023$ , and therefore the orbital contribution is zero, the splitting of any  $S$  manifold is as in Fig. 1.16(A) and independent of the orientation of the molecule with respect to the external magnetic field; when there is an orbital contribution, a different splitting of the  $S$  manifold in any direction occurs (Figs. 1.16(B) and 1.16(C)), and upon rapid rotation there is an average splitting of the levels.

Besides providing a different effective magnetic moment for each orientation, spin-orbit coupling is also able to cause a splitting of an  $S$  manifold with  $S > \frac{1}{2}$  at zero magnetic field. When  $S$  is, let us say,  $\frac{3}{2}$ , spin-orbit coupling and low symmetry

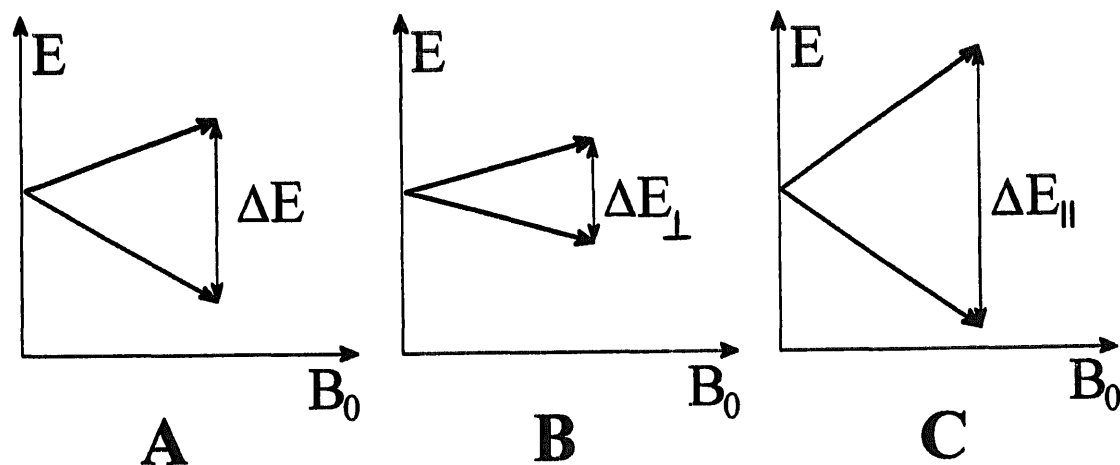


Fig. 1.16. The splitting of the  $S = \frac{1}{2}$  manifold in a magnetic field  $B_0$  when (A)  $g$  is isotropic and there are only two energy values independent of the orientation of the molecule in the magnetic field and (B, C) the energies depend on the orientation of the molecule in the magnetic field ( $\Delta E_{\parallel} > \Delta E_{\perp}$ ).

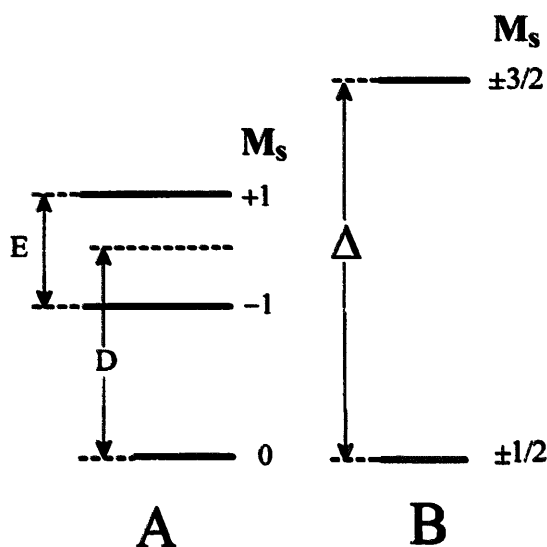


Fig. 1.17. The splitting of an  $S = 1$  (A) and  $S = \frac{3}{2}$  (B) manifold in the presence of spin orbit coupling and low symmetry components.  $D$  is the axial and  $E$  the rhombic ZFS parameter (the latter only shown in case (A)). The wavefunctions are labeled as high field eigenfunctions.

effects split the quartet in a way similar to that depicted in Fig. 1.12. When  $S$  is half integer, at least two-fold degeneracies remain (so called Kramers doublets,  $M_S = \pm n/2$ ), whereas when  $S$  is integer the splitting can remove any degeneracy (Fig. 1.17).

Such splitting is called zero field splitting and indicated as ZFS. It adds up to the Zeeman energy. In the spin-Hamiltonian formalism, i.e. when the effects of the orbital angular momentum are parameterized, it is indicated as

$$\mathcal{H} = \mathbf{S} \cdot \mathbf{D} \cdot \mathbf{S} \quad (1.24)$$

where  $\mathbf{D}$  is the ZFS tensor. It is traceless, in the sense that its effect upon rapid rotation is zero (rapid means that the rotation rate ( $s^{-1}$ ) is larger than the maximum energy splitting ( $\Delta E/h$  ( $s^{-1}$ )). However, its appearance is of paramount importance in electron relaxation and in determining the magnetic properties of metal complexes. The comparison of Fig. 1.12 with Fig. 1.17(B) shows that the nuclear quadrupole splitting and the ZFS are formally similar. When the splitting is less than axial, the ZFS is defined by two parameters,  $D$  and  $E$  (Fig. 1.17).

Hamiltonian (1.24) is formally equivalent to that describing the interaction between two spins  $s_1$  and  $s_2$  whose sum is  $S$ . Actually, in organic radicals where spin-orbit interactions are negligibly small, the interactions between the two electron spins in an  $S = 1$  system cause ZFS.

### 1.5. About the energies

Up to now we have seen that  $S$  or  $I$  manifolds split in an external magnetic field according to their  $M_S$  or  $M_I$  values. The latter are the allowed components of the  $S$

or  $I$  vectors along the external magnetic field. When we said that the spins orient in a magnetic field as in Fig. 1.5 we actually referred to the low energy orientation, which is the only populated at  $T = 0$  K. The excited levels are separated by the Zeeman energy. Such energies are about  $0.3 \text{ cm}^{-1}$  at 0.3 T for the electron, and 658 times smaller for the proton. The thermal energy  $kT$  is about  $200 \text{ cm}^{-1}$  at 300 K and about  $0.7 \text{ cm}^{-1}$  at 1 K. So, the population of the two levels is almost the same at every temperature above a few kelvin. The Boltzmann population  $P_i$  of each  $M_I$  level is

$$P_i = \frac{\exp(-E_i/kT)}{\sum_i \exp(-E_i/kT)} \quad (1.25)$$

where  $E_i$  is the energy of the  $i$ th level with respect to the ground level and the sum is extended to all levels, each weighted by its energy. When  $kT \gg E_i$ , as happens at room temperature,  $E_i/kT$  tends to zero, the exponential tends to unity and each level is almost equally populated. The magnetic resonance experiments are based on the small population differences. The energy of the system (for instance, an ensemble of  $N_A$  spins) is given by the sum of the energies for each level weighted by the population of the level.

### 1.6. Magnetization and magnetic susceptibility

The effect of the external magnetic field is that of splitting the energies of the  $S$  or  $I$  manifolds (see, for example, Figs. 1.6 and 1.9) and, therefore, of making different the populations of the levels. The difference in population according to the Boltzmann law (Eq. (1.25)) tells us that the magnetic field has indeed changed the energy of the system. By making reference for simplicity to Fig. 1.6 (two orientations), the spins with the lower energy orientation are more than those with the higher energy orientation. As a consequence, an induced magnetic moment  $\mu_{\text{ind}}$  is established. The net interaction energy of the whole system with the magnetic field is the product of the induced magnetic moment and the magnetic field. The magnetization per unit volume  $M$  (Eq. (1.2)) corresponds to the induced magnetic moment per unit volume and, for many substances, is found to be proportional to the applied magnetic field  $B_0$ :

$$M = \frac{\mu_{\text{ind}}}{V} = \chi_V H = \frac{1}{\mu_0} \chi_V B_0 \quad (1.26)$$

where  $\chi_V$ , the dimensionless proportionality constant between  $M$  and  $H$ , is the magnetic susceptibility per unit volume.

Classically, this effect can be seen as an ensemble of magnetic moments randomly oriented in the absence of a magnetic field with resultant equal to zero. When an external magnetic field is applied, it tends to orient the magnetic moments and to provide a resultant different from zero (Fig. 1.18). The larger the magnetic field, the larger the resultant induced magnetic moment. From Eq. (1.26),  $\chi_V = \mu_0 M/B_0 =$

$\mu_0\mu_{\text{ind}}/(B_0V)$ : for  $N_A$  particles,  $\mu_{\text{ind}} = N_A\langle\mu\rangle$ , where  $\langle\mu\rangle$  is the average induced magnetic moment per particle (see later), and

$$\chi_M = V_M\chi_V = V_M \frac{\mu_0 M}{B_0} = \frac{\mu_0 N_A \langle\mu\rangle}{B_0} \quad (1.27)$$

where  $\chi_M$  ( $\text{m}^3 \text{mol}^{-1}$ ) is the magnetic susceptibility per mole, and  $V_M$  is the molar volume.  $\chi_M$  is magnetic field independent, just like  $\chi_V$ .

Let us now take an  $S$  manifold, unsplit at zero magnetic field, with no orbital angular momentum. The sum of the energies in a magnetic field would be zero (Eq. 1.19) if the levels were equally populated:

$$E = g_e\mu_B B_0 \sum_{M_S=-S}^{M_S=S} M_S = 0 \quad (1.28)$$

However, if the populations are considered (see, for example, Fig. 1.18 for  $S = \frac{1}{2}$ ), in an ensemble of  $N_A$  particles, and by recalling that  $M_S = \langle S, M_S | S_z | S, M_S \rangle$  (Eq. (1.7)), the energy is

$$E = N_A g_e \mu_B B_0 \frac{\sum \langle S, M_S | S_z | S, M_S \rangle \exp(-g_e \mu_B B_0 M_S / kT)}{\sum \exp(-g_e \mu_B B_0 M_S / kT)} \quad (1.29)$$

If we consider that  $g_e \mu_B B_0 M_S \ll kT$ , the exponential is just  $(1 - g_e \mu_B B_0 M_S / kT)$ . It follows from Eq. (1.28) that the denominator is just  $2S + 1$ , and the energy is given

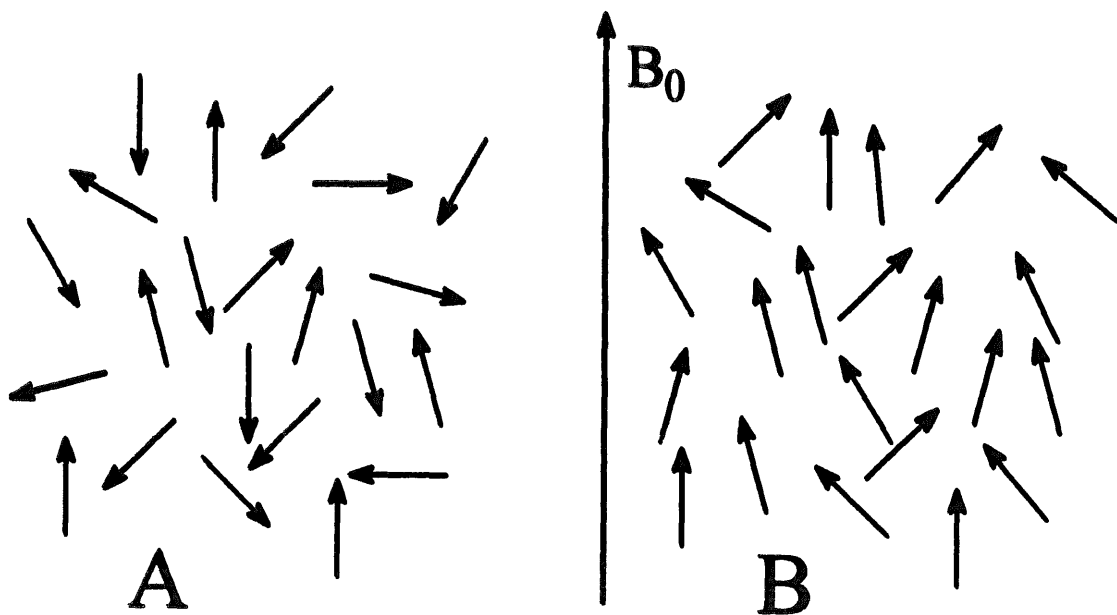


Fig. 1.18. An ensemble of  $S = \frac{1}{2}$  magnetic moments (A) orient themselves along the allowed directions when a magnetic field is applied (B). The partial orientation determines a resultant non-zero magnetic moment.



by

$$E = -N_A g_e^2 \mu_B^2 \frac{S(S+1)B_0^2}{3kT} = N_A g_e \mu_B B_0 \langle S_z \rangle \quad (1.30)$$

The quantity

$$\langle S_z \rangle = \frac{\sum \langle S, M_S | S_z | S, M_S \rangle \exp(-g_e \mu_B B_0 M_S / kT)}{\sum \exp(-g_e \mu_B B_0 M_S / kT)} = -\frac{g_e \mu_B S(S+1)B_0}{3kT} \quad (1.31)$$

is called the expectation value of  $S_z$ . By operating with  $S_z$  on each  $|S, M_S\rangle$  level, considering the population, and summing up over all the levels, we obtain an expectation value different from zero.

In contrast, from the classical treatment, the energy of the system is also given by the product of the induced magnetic moment along the field,  $\mu_{\text{ind}}$  ( $\mu_{\text{ind}} = N_A \langle \mu \rangle$ , see Eqs. (1.26) and (1.27)) and the external magnetic field  $B_0$  (cf. Eq. (1.3)):

$$E = -\mu_{\text{ind}} B_0 \quad (1.32)$$

Therefore, by combining Eqs. (1.30) and (1.32):

$$\langle \mu \rangle = \frac{\mu_{\text{ind}}}{N_A} = \mu_B^2 g_e^2 \frac{S(S+1)B_0}{3kT} = -\mu_B g_e \langle S_z \rangle \quad (1.33)$$

In other words, the induced magnetic moment per particle is just proportional to the expectation value  $\langle S_z \rangle$ . Note that the value of  $\langle S_z \rangle$  is referred to a single spin  $S$  and to its fractional occupancy of the energy level ladder. In the case of a spin ensemble, the value of  $\langle S_z \rangle$  provides the average value of  $S_z$  of the ensemble.  $\langle S_z \rangle$  is a dimensionless number. From Eqs. (1.27) and (1.33), the magnetic susceptibility per mole is given by

$$\chi_M = \mu_0 N_A \mu_B^2 g_e^2 \frac{S(S+1)}{3kT} \quad (1.34)$$

By using Eq. (1.8) we obtain

$$\chi_M = \mu_0 N_A \frac{\mu_S^2}{3kT} \quad (1.35)$$

This result of the quantum mechanical treatment coincides with the derivation of magnetic susceptibility in terms of classical magnetic moments if their moduli are taken equal to those associated to the individual spins.

All the above treatment holds for a single  $S$  manifold. If there is some orbital contribution to the magnetic moment, it cannot be neglected. All the calculations should be repeated by using Hamiltonian (1.20) for a generic direction  $k$  and, by

keeping in mind (Eq. (1.27)) that  $\chi_M = \mu_0 N_A \langle \mu \rangle / B_0$

$$\chi_{M_{kk}} = - \frac{\mu_0 N_A \mu_B}{B_0} \frac{\sum_i \langle \phi_i | L_{kk} + g_e S_{kk} | \phi_i \rangle \exp(-E_i/kT)}{\sum_i \exp(-E_i/kT)} \quad (1.36)$$

where the sum is over all the levels of the  $S$  manifold now containing the orbital part.  $E_i$  is the Zeeman energy and may also contain ZFS effects. In the spin-Hamiltonian formalism, neglecting ZFS effects

$$\langle \phi | L_{kk} + g_e S_{kk} | \phi \rangle = g_{kk} M_S \quad (1.37)$$

and

$$\chi_{M_{kk}} = \mu_0 N_A \mu_B^2 g_{kk}^2 \frac{S(S+1)}{3kT} \quad (1.38)$$

where  $g_{kk}$  is now different from  $g_e$  (Eq. (1.21)).  $\chi_M$  is now a tensorial quantity.

Eq. (1.36) is called the Van Vleck equation. In that form the Zeeman operator operates only to first order. Indeed, we should include the second order Zeeman term, which allows the interaction between the ground  $S$  multiplet ( $\phi_i$  functions) with all the excited ones ( $\phi_j$  functions):

$$\sum_{j \neq i} \frac{\mu_B^2 |\langle \phi_i | L_{kk} + g_e S_{kk} | \phi_j \rangle|^2}{E_i^0 - E_j^0} \quad (1.39)$$

where  $E_i^0$  and  $E_j^0$  are the energies at zero magnetic field. The complete Van Vleck equation, including the population, is

$$\chi_{M_{kk}} = \mu_0 N_A \mu_B^2 \times \frac{\sum_i \left[ \frac{|\langle \phi_i | L_{kk} + g_e S_{kk} | \phi_i \rangle|^2}{kT} - 2 \sum_{j \neq i} \frac{|\langle \phi_i | L_{kk} + g_e S_{kk} | \phi_j \rangle|^2}{E_i^0 - E_j^0} \right] \exp(-E_i^0/kT)}{\sum_i \exp(-E_i^0/kT)} \quad (1.40)$$

## 1.7. The nuclear magnetic resonance experiment

The small difference in population among the  $M_I$  or  $M_S$  levels allows the magnetic resonance experiments. From now on we will focus on the nuclear magnetic resonance experiment, but little would be changed if we dealt with EPR.

### 1.7.1. The continuous wave experiment and definition of $T_1$ and $T_2$

The magnetic resonance phenomenon was first observed through a continuous wave experiment [2]. Resonance between the two  $M_I$  levels of an  $I = \frac{1}{2}$  nucleus in a magnetic field (without loss of generality) can be achieved by applying a magnetic

field rotating with a frequency (see Eq. (1.16)) such that

$$h\nu = \hbar\omega = \mu_N |g_I| B_0 = \hbar |\gamma_I| B_0 \quad (1.41)$$

The frequency  $\nu$  is in the radiofrequency (r.f.) range; for the proton it is 100 MHz at 2.3 T. In order to excite the transition, the radiation should be polarized orthogonally to the external magnetic field. The radiation stimulates upward and downward transitions equally. The difference in population accounts for a net absorption of energy. The r.f. therefore tends to bring the two levels to equal populations. When this situation is reached, we have saturation of the signal. No net absorption can be observed. The non-radiative processes which tend to bring back the system to equilibrium tend to re-establish the difference in population. Such processes provide exchange of energy between the spin system and the surrounding, which is called lattice. As described in more detail in Section 1.7.4, the achievement of the equilibrium from non-equilibrium conditions is often assumed to occur through exponential processes of the type

$$\begin{aligned} \exp(-t/T_1) \quad \text{and} \quad \exp(-t/T_2) \quad \text{or} \\ \exp(-R_1 t) \quad \text{and} \quad \exp(-R_2 t) \end{aligned} \quad (1.42)$$

where the time constants  $T_1$  and  $T_2$  are called longitudinal and transverse relaxation times.  $T_1^{-1}$  and  $T_2^{-1}$  are the corresponding rate constants, indicated as  $R_1$  and  $R_2$ . Traditionally, NMR spectroscopists are bound to the relaxation times, although the use of relaxation rates is more convenient.

The difference in population between the two levels ensures the establishment of a magnetic moment along the  $z$  direction defined by the external magnetic field. This is the magnetic moment that we have described in detail for the electron in Section 1.6. Such a magnetic moment can be thought to be the component of a single macroscopic magnetic moment precessing about  $z$ . In other words, an ensemble of spins  $\frac{1}{2}$  will be a little more than 50% precessing about  $z$  with  $M_I = \frac{1}{2}$  and a little less than 50% precessing about  $-z$  with  $M_I = -\frac{1}{2}$ . The difference will provide the magnetic moment along  $z$ , which could be thought of as being due to a number of spins equal to the excess spins, all rotating in phase (i.e. represented by coincident vectors). Such a resulting macroscopic rotating vector has the following components:

$$M_z = \text{constant} \quad (1.43)$$

$$M_y = M_0 \cos \omega t \quad (1.44)$$

$$M_x = M_0 \sin \omega t \quad (1.45)$$

The time average component in the  $xy$  plane is zero. The frequency  $\omega$  is the frequency of precession about  $z$  and is the resonance frequency ( $\omega = 2\pi\nu$ ). Indeed, if we send r.f. with exactly that frequency, the vector senses the external magnetic field as well as the r.f. field. The magnetization vector undergoes a spiral-type movement which brings its  $z$  component from  $M_z$  to  $-M_z$  (Fig. 1.19). If we use as reference frame a rotating coordinate system with  $z'$  coinciding with  $z$  and  $x'$  and  $y'$  rotating

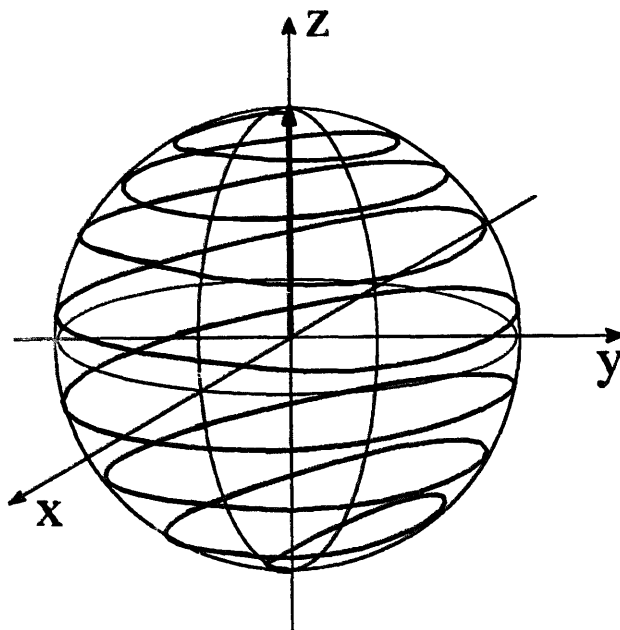


Fig. 1.19. The spiral-type movement of the macroscopic magnetization vector subject to the simultaneous action of an external static magnetic field and of an r.f. field rotating at the resonance frequency.

at the  $\omega$  frequency, the magnetization vector will be still in the new coordinate frame. The r.f. field rotating at frequency  $\omega$  will also be a constant vector. In the rotating frame the magnetization vector only precesses about the r.f. field (Fig. 1.20).

Before the appropriate r.f. is turned on, the magnetization vector has an equilibrium component  $M_z$  along  $z$  and zero value in the  $xy$  plane. The r.f. decreases the  $M_z$  value and establishes an  $M_{xy}$  different from zero. The return to equilibrium can be followed along  $z$ , thus defining  $T_1$ , and in the  $xy$  plane, thus defining  $T_2$ . The two processes are different. To the longitudinal process, only energy exchanges with the lattice through switches of energy levels contribute. The longitudinal relaxation time is also called spin lattice relaxation time. Spin–spin flip-flop transitions not involving energy exchange do contribute to  $R_2$ . For this reason the transverse relaxation time is also called spin–spin relaxation. Because all processes contributing to  $R_1$  also contribute to  $R_2$ , but not vice versa, the relation

$$R_2 \geq R_1 \quad (1.46)$$

always holds.

### 1.7.2. The pulse experiment

If we send a radiation for a time short with respect to  $T_1$  or  $T_2$ , but with enough power to affect the spin system, we say that we send a pulse. Let us say that the pulse is at the frequency  $\omega$  of the rotating frame. The magnetization vector starts precessing about the r.f. field. The precession will continue with time, at least for times shorter than  $T_1$  and  $T_2$ , with an angular velocity proportional to the r.f. field,

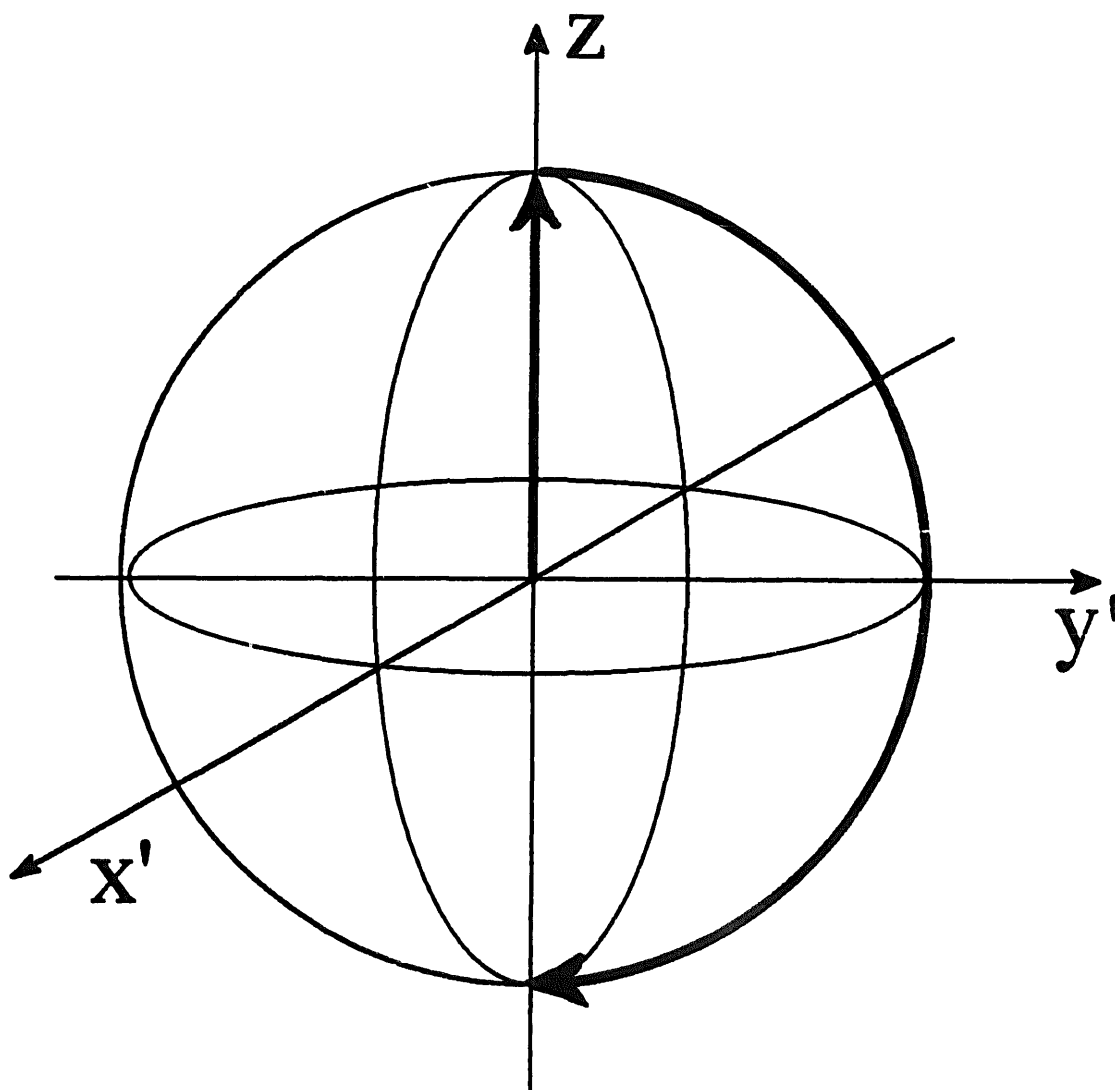


Fig. 1.20. The spiral movement of the macroscopic magnetization becomes a rotation about the  $x'$  (or  $y'$ ) axis of the rotating frame if the sphere rotates about  $z$  with the proper frequency.

i.e. to the power of the pulse. The rotation angle after a given time will thus depend on the product of power and time, i.e. on the energy of the pulse. If the r.f. field is along  $x'$  in the rotating frame, the magnetization vector will rotate about  $x'$  towards  $y'$ . After a given time, let us say when the rotation is  $90^\circ$ , we stop the pulse and we let the system return to equilibrium. The coil which transmitted the pulse reveals now the disappearance of the magnetization in the  $xy$  plane. We say that the coil reveals the free induction decay (FID). The process is exponential with time constant  $T_2$  (Fig. 1.21). The cosine Fourier transform of this exponential decay is

$$\int_0^\infty \exp(-t/T_2) \cos(\omega t) dt = \frac{T_2}{1 + \omega^2 T_2^2} \quad (1.47)$$

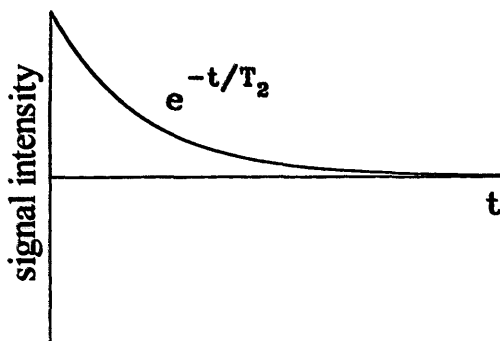


Fig. 1.21. The FID detected on resonance with the precession frequency of the signal of interest.

The frequency function is a Lorentzian with linewidth at half height of  $(\pi T_2)^{-1}$  ( $= R_2/\pi$ ). The same, of course, holds in the continuous wave experiment.  $R_2$  is a measure of the uncertainty of the energy levels, which gives the linewidth in every spectroscopy. The uncertainty principle, according to which the uncertainty in energy of a level is inversely proportional to the lifetime, tells us that  $T_2$  is a measure of the lifetime of the energy levels.

If the frequency of the pulse is different from the resonating frequency, nothing changes as long as the pulse contains the latter frequency as a component. It can be shown that a pulse effectively covers an interval of frequencies of the order of the reciprocal of the pulse length, centered at its own frequency (carrier frequency). The FID now has the shape shown in Fig. 1.22; besides intensity and linewidth, it contains the information about the nuclear resonance frequency.

### 1.7.3. The chemical shift

The effective magnetic field which a nuclear spin senses when placed in an external magnetic field is the sum of several contributions, whose nature is not discussed here except for that due to the interaction with unpaired electron(s). For example, the paired electrons will decrease the external magnetic field, since they experience an

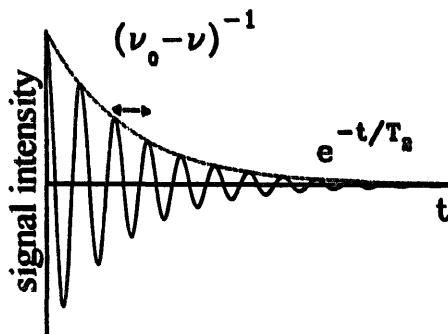


Fig. 1.22. The FID detected off resonance with respect to the precession frequency of the signal of interest. The FID has the shape of a damped oscillation, where the time separation between adjacent maxima equals the reciprocal of the difference  $\nu_0 - \nu$ .

induced magnetic field which opposes to the external magnetic field. This is the same phenomenon which gives rise to bulk diamagnetism. Therefore, all nuclei in a diamagnetic molecule will experience a magnetic field smaller than free nuclei. Since free nuclei are not a practical standard, nuclei in convenient chemical compounds are used as standards. Typically, tetramethylsilane (TMS) is used in proton NMR because its protons are surrounded by a relatively large amount of paired electrons and essentially are at an extreme of the range. The effective magnetic field sensed by such protons is

$$B = B_0(1 - \sigma_{\text{TMS}}) \quad (1.48)$$

where  $\sigma$  is the so-called shielding constant and  $B_0\sigma$  is the induced magnetic field which opposes to  $B_0$  (see also Eq. (1.2)). The proton of  $\text{CHCl}_3$  will experience a smaller shielding constant because chlorine, being quite electronegative, will attract the electrons and remove them from the proton. So, the proton of  $\text{CHCl}_3$  will sense a larger effective magnetic field than the protons of TMS when placed in the same magnetic field (Fig. 1.23).

For fixed  $B_0$ , the frequency needed to have the transition will be larger for  $\text{CHCl}_3$  than for TMS. The difference in frequency is called chemical shift with respect to TMS. In this case the shift is positive:

$$\Delta\nu = \nu_{\text{CHCl}_3} - \nu_{\text{TMS}} \quad (1.49)$$

We sometimes say that the  $\text{CHCl}_3$  proton resonates downfield (at a smaller external magnetic field) with respect to TMS, which in turn resonates upfield (at a larger external magnetic field) if we imagine to keep the frequency fixed and to vary the magnetic field.

Under the above definition the chemical shift is expressed in frequency units (hertz) and depends on the external magnetic field, which then needs to be specified. It may be convenient to express the chemical shift as a pure number, i.e. divided by the

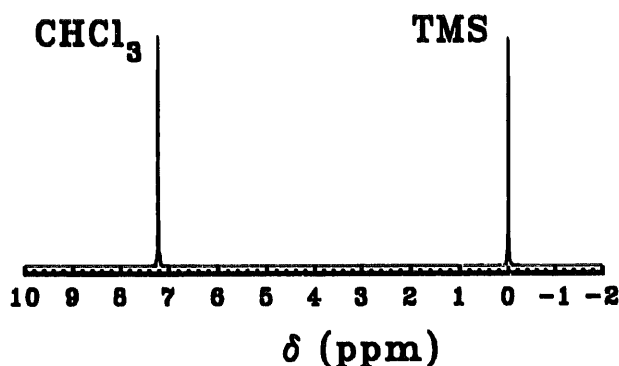


Fig. 1.23. NMR spectrum of a mixture of  $\text{CHCl}_3$  and TMS taken at 600 MHz proton Larmor frequency. By taking the chemical shift of TMS as zero, the chemical shift of  $\text{CHCl}_3$  is 7.28 ppm. Shifts to the left of TMS are taken as positive and called downfield. At the chosen magnetic field, the chemical shift of  $\text{CHCl}_3$  is 4326 Hz.

frequency of the standard:

$$\frac{\Delta\nu}{\nu_0} = \delta = \frac{\nu_{\text{CHCl}_3} - \nu_{\text{TMS}}}{\nu_{\text{TMS}}} = 7.28 \times 10^{-6} = 7.28 \text{ ppm} \quad (1.50)$$

where  $\nu_0$  is the frequency of the spectrometer magnetic field referred to the standard and ppm means parts per million. The symbol  $\delta$  will be used for chemical shift throughout the book, and all chemical shift equations will be expressed in  $\delta$ .

Unpaired electrons will have a preference for being aligned along the external magnetic field, in the absence of other restrictions. Therefore, their magnetic moment will sum up and increase the effective magnetic field sensed by a nucleus. The interaction between a magnetic nucleus and unpaired electrons is called hyperfine coupling, after Fermi's account of the hyperfine splitting of the lines in the atomic spectra due to the coupling between the proton and the unpaired electron [3]. The shift in this case is positive (i.e. downfield: since there is the contribution of the electron dipole, a smaller external field is needed to bring the nucleus to resonance). The effect of the presence of unpaired electrons on the nuclear properties will be the subject of this book and of course will be discussed in detail, hopefully in a clear, concise and exhaustive way.

In terms of the Hamiltonian, such hyperfine coupling is represented as

$$\mathcal{H} = I \cdot A \cdot S \quad (1.51)$$

where  $A$  is the hyperfine coupling tensor. It is a tensor because it has different values depending on the orientation of the molecular frame within an external magnetic field, which defines the laboratory  $z$  axis (see Chapter 2).

#### 1.7.4. Something more about relaxation rates

$T_1$  and  $T_2$  have already been defined in Section 1.7.1. Since their understanding is fundamental to any approach to NMR experiments and theory, we repeat here the definitions by using a different wording. When an ensemble of independent and equivalent spins at equilibrium in a magnetic field is perturbed, for example by irradiation at the right frequency or by suddenly changing the magnetic field, the system is not at equilibrium any longer. For simplicity we like to consider the spins independent, i.e. not interacting one another. This assumption is convenient to define  $T_1$  but unrealistic, as we will see in the following chapters. The spins are also assumed to experience the same chemical shift. If we refer to the Boltzmann law, which accounts for the levels' population, we can say that, after a perturbation, the spin temperature is different from the lattice temperature. For lattice we mean the environment of the nuclei, which is assumed to have an infinite heat capacity.

After the perturbation, the system tends to reach equilibrium again. We assume that the return to equilibrium is a stochastic process, i.e. each step towards equilibrium is random and uncorrelated to other steps. Under these conditions the return to equilibrium is a first order kinetic process. The decay, as in Eq. (1.42), is then



given by

$$F(t) = \exp(-Rt) \quad (1.52)$$

where  $t$  is the time and  $R$  is a rate constant, as anticipated in Section 1.7.1.

The magnetic field has cylindrical symmetry, i.e. the physical properties of a system do not change upon rotation about the field direction, and there is no difference between  $x$  and  $y$  directions. If the measurement of the return to equilibrium is performed along the  $B_0$  direction, i.e. the return to equilibrium of  $M_z$  is followed, the rate constant is said to be longitudinal and is indicated as  $R_1$ . The magnetization reaches equilibrium through transitions between pairs of levels differing by  $\Delta M_I$  or  $\Delta M_S = \pm 1$ . Such transitions are induced, like in the magnetic resonance experiments, by oscillating magnetic fields available within the lattice. Matter, even in the condensed phase, experiences continuous movements whose average kinetic energy is proportional to  $kT/2$  for each degree of freedom. Matter contains magnetic dipoles, electric charges, etc. which are capable of originating magnetic fields upon sudden reorientations or sudden movements which can be seen as short pulses. Longitudinal relaxation occurs through energy exchange with the lattice until the equilibrium population of the levels is obtained and the spin temperature equals the lattice temperature. We recall that the lattice is assumed to have an infinite heat capacity.

In a typical experiment, called inversion recovery,  $M_z$  is initially inverted by applying a  $180^\circ$  pulse. Its recovery along the  $z$  axis is given by

$$M_z(t) = M_z(\infty) - 2M_z(\infty) \exp(-R_1 t) \quad (1.53)$$

where  $M_z(\infty)$  is the equilibrium value of  $M_z$ . The value of  $M_z(t)$  at various times  $t$  is sampled by applying a  $90^\circ$  pulse and measuring the intensity of the detected signal.  $R_1$  can then be extracted from a fitting of the data to an exponential recovery.

If the rate of reaching equilibrium is measured orthogonally to the magnetic field, i.e. by sampling the projection of the magnetization in the  $xy$  plane obtained, for instance, after a  $90^\circ$  pulse, a different rate constant is obtained, which is called the transverse relaxation rate and indicated as  $R_2$ . In a pulsed experiment, the rate of reaching equilibrium is equal to the rate of disappearance of magnetization in the  $xy$  plane, and is proportional to the linewidth at half height:

$$\pi \Delta\nu_{1/2} = R_2 \quad (1.54)$$

All the mechanisms which contribute to  $R_1$  contribute also to  $R_2$ , because the re-establishment of the equilibrium population brings zero magnetization in the  $xy$  plane. The dephasing, or fanning out, of the single spin components in the  $xy$  plane contributes only to  $R_2$ . Therefore

$$R_2 > R_1 \quad \text{or} \quad R_2 = R_1 + c \quad (1.55)$$

where  $c$  is the cumulative rate of all processes which lead to the disappearance of the magnetization in the  $xy$  plane besides those which lead to the re-establishment of Boltzmann equilibrium. Typically, local magnetic fields oscillating along  $B_0$  at any frequency close to zero produce oscillations in the actual magnetic field and

increase the linewidths; in other words, such fields  $b_z$  spread the spin moments (Fig. 1.24) through the vectorial interaction with the  $xy$  magnetization:

$$b_z \times M_{xy} \quad (1.56)$$

The dephasing of the single spins leads to the equilibrium value of the magnetization in the  $xy$  plane, which is zero. We have already seen that the simultaneous change of orientation of two spins contributes only to  $R_2$ . Besides measuring the linewidth, typical experiments for measuring  $R_2$  are the so-called spin-echo experiments. In their simplest form, a  $90^\circ$  pulse is applied first, followed by a  $180^\circ$  pulse after a variable time  $t$ . The intensity of the signal is measured after another time  $t$  following the  $180^\circ$  pulse.

In another type of experiment, the magnetization is kept locked in the  $xy$  plane. A  $90^\circ$  pulse with  $B_1$  along  $y$  (in the rotating frame) sends the magnetization along  $x$ . Then  $B_1$  is aligned along  $x$  (Fig. 1.25). The field  $B_1$  originated by the transmitter is the only field sensed by the magnetization in the rotating frame. Then the magnetization precesses along  $B_1$ . At equilibrium the magnetization will return along  $z$ . The time constant for the kinetic process of returning to equilibrium, i.e. for the

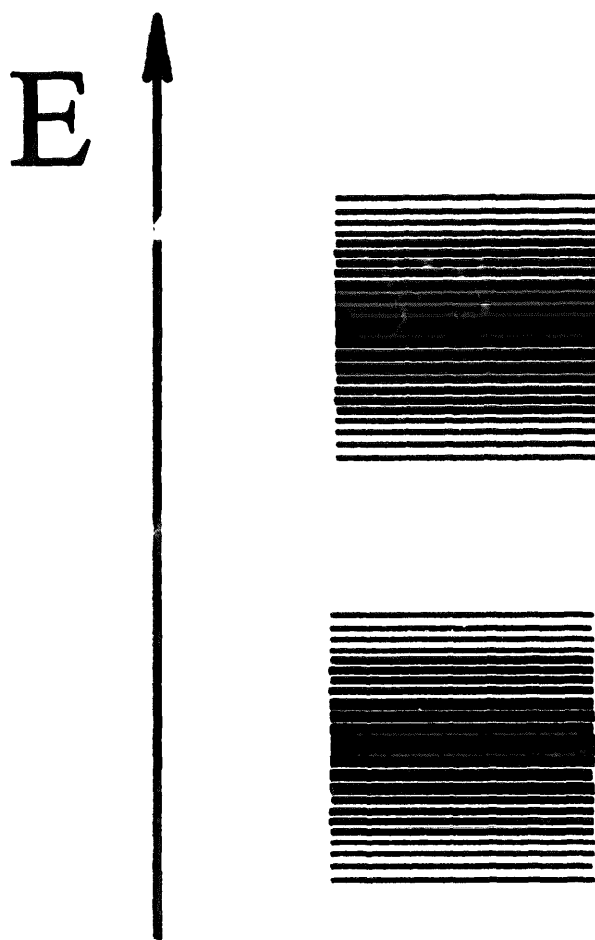


Fig. 1.24. The spreading of energy levels as due to an effective fluctuating magnetic field along  $z$ .

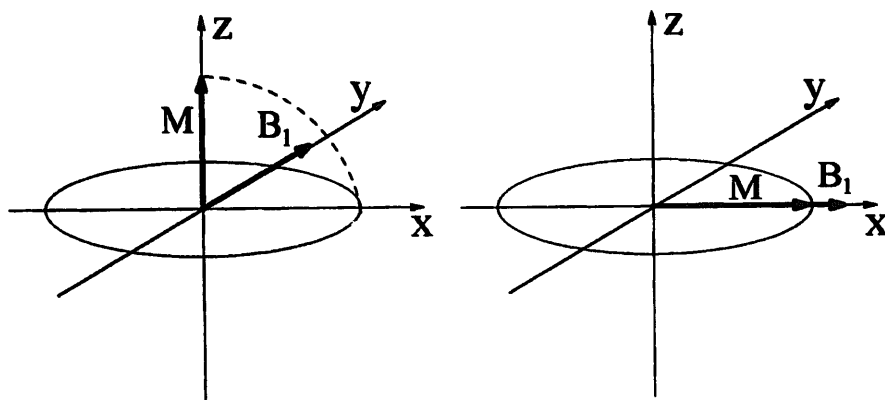


Fig. 1.25. In a spin-locking experiment the magnetization is initially brought along the  $x$  axis of the rotating frame (left), and then *locked* along that axis (right), by proper reorientation of the r.f. field  $B_1$ .

disappearance of the magnetization along  $y$  when a spin-locking field  $B_1$  is operating, is called  $T_{1\rho}$  and the corresponding constant is called  $R_{1\rho}$ .

The presence of unpaired electrons will activate new relaxation pathways, and we will have a nuclear  $R_i$  ( $i = 1$  or  $2$ ) enhancement which is indicated as  $R_{iM}$ . Similarly,  $R_{1\rho}$  also increases. This is what will be treated in some detail in Chapter 3.

We should end this section by recalling that, while the concept of relaxation is very general, the concept of relaxation rates is much less general, as it implies exponential return to equilibrium of magnetization. Exponential relaxation can only occur when the spin system is weakly coupled to the lattice, and the latter can be assumed to have infinite heat capacity. However, in the case of nuclei, very often the lattice is also constituted by other nuclear spin systems that have a limited heat capacity, of the same order as that of the spin system under investigation. In the case of electron spins, sometimes the coupling with the lattice is too strong, and non-exponential relaxation may also occur. These concepts will be further developed in Chapters 3 and 6. Despite these drawbacks, the concept of relaxation rates is still very useful and is thoroughly used, especially when dealing with nuclear relaxation rate enhancements due to unpaired electrons which, as we will see, are often truly exponential contributions.

## References

- [1] S.H. Koenig, A.G. Prodel and P. Kusch, *Phys. Rev.*, 88 (1952) 191.
- [2] F. Bloch, W.W. Hansen and M. Packard, *Phys. Rev.*, 69 (1946) 127; F. Bloch, *Phys. Rev.*, 70 (1946) 460; F. Bloch, W.W. Hansen and M. Packard, *Phys. Rev.*, 70 (1946) 474; E.M. Purcell, H.C. Torrey and R.V. Pound, *Phys. Rev.*, 69 (1946) 37; E.M. Purcell, *Phys. Rev.*, 69 (1946) 681.
- [3] E. Fermi, *Z. Phys.*, 60 (1930) 320.

## General references

For the physical concepts we have mainly referred to B.I. Bleaney and B. Bleaney, *Electricity and Magnetism*, Oxford University Press, 3rd edn., 1976.

For the CW NMR experiments one can refer, among others, to: J.A. Pople, W.G. Schneider and H.J. Bernstein, *High-Resolution Nuclear Magnetic Resonance*, McGraw-Hill, New York, 1959.

There are numerous books on FT-NMR. The reference book is: R.R. Ernst, G. Bodenhausen and A. Wokaun, *Principles of Nuclear Magnetic Resonance in One and Two Dimensions*, Oxford University Press, Oxford, 1987. We may also indicate: T.C. Farrar and E.D. Becker, *Introduction to Pulse and Fourier Transform NMR Methods*, Academic Press, New York, 1971.

Previous books on NMR of paramagnetic molecules are: G.N. La Mar, W.DeW. Horrocks, Jr. and R.H. Holm (Eds.), *NMR of Paramagnetic Molecules*, Academic Press, New York, 1973. I. Bertini and C. Luchinat, *NMR of Paramagnetic Molecules in Biological Systems*, Benjamin-Cummings, Menlo Park, 1986.